Biosensors and Bioelectronics 27 (2011) 172–177

Contents lists available at ScienceDirect

Biosensors and Bioelectronics

journal homepage: www.elsevier.com/locate/bios

A valuable visual colorimetric and electrochemical biosensor for porphyrin

Xiaoquan Lu*, Dongxia Zhao, Zhengen Song, Bowan Wu, Bingzhang Lu, Xibin Zhou, Zhonghua Xue

Key Laboratory of Bioelectrochemistry and Environmental Analysis of Gansu Province, College of Chemistry and Chemical Engineering, Northwest Normal University, Lanzhou 730070, China

ARTICLE INFO

Article history:
Received 29 March 2011
Received in revised form 27 June 2011
Accepted 28 June 2011
Available online 6 July 2011

Keywords:
Self-assembled monolayer
Biosensor
Porphyrin
Visual colorimetry
Electrochemistry

ABSTRACT

Porphyrin is able to specifically combine with phosphorus, thus a novel bifunctional sensing platform for determination of porphyrin by visual colorimetry and electrochemistry was demonstrated. A pretreated gold sheet (or electrode) with 2-mercatpoethanol (2-ME) was chemically modified by $POCl_3$ to obtain the surface phosphate active sites. The different stages of modified electrode were characterized by electrochemical impedance spectroscopy (EIS). The 1:1 cationic sitting-atop (SAT) complex P(V)–porphyrin was formed due to the high affinity of the modified gold sheet (or electrode) towards the porphyrin, resulting in electron transfer resistance increase of the electrode surface. Meanwhile, a dramatic color changing from burgundy to dark green of porphyrin solution was observed with the naked-eye within 3 s. What's more, this was reflected by the notable change of the Soret band of porphyrin when using UV–vis. Two sensing systems provide different sensitivity for porphyrin analysis. With visual colorimetry, porphyrin can be detected at a level of 1.0×10^{-6} M, whereas the detection limit of porphyrin is 3.0×10^{-8} M using the EIS method. The practical application of the sensor to determination of pheophytin which was obtained from fresh spinach leaves has been accomplished. The results demonstrate the facility and effectivity of our introduced bifunctional biosensor for quantitative analysis of porphyrin.

1. Introduction

The self-assembled monolayers (SAMs) have received extensive attention over the past decades (Schönherr et al., 1997; Stettner and Winkler, 2010; Sun et al., 2008). In particular, thiols on gold have been well studied and regarded as model systems for a variety of applications for elaborate designs of molecular-based electronics, tailored sensor surfaces, and nanopatterning (Carroll and Christopher, 2002; Chiu et al., 2009; Seitz et al., 2009). The interest in using these functional SAMs has led to the development of chemical sensors for detection of biomolecules and various ions in vitro and vivo studies. For example, Fragoso et al. prepared SAMs of dithiolated aromatic scaffolds on gold for the label-free detection of prostate-specific antigen using EIS (Fragoso et al., 2008). Rezaei and co-workers developed an electrochemical impedimetric immunosensor for determination of insulin-like growth factor-1 based on SAMs (Rezaei et al., 2011). Impedimetric biosensor for the monitoring of the clotting activity of rennet has been investigated as well (Panagopoulou et al., 2010). Recently, our group developed a new type of receptor for dihydrogenphosphate anion recognition through SAMs of thiol-derivatized porphyrins on Au substrate (Zhi et al., 2009). However, specific phosphate-based SAM sensor for detecting the porphyrin that exists widely in nature is greatly needed due to SAMs' flexible design, simple operation, fast response, high sensitivity and selectivity as sensors.

Porphyrin and its derivatives, such as chlorophyll, pheophytin, vitamin B_{12}, hemoglobin and myoglobin are expected to play key roles in biological (cellular respiration, photosynthesis) and biomimetic (solar cell) systems. Their excellent stability and unique optical/electronic properties make them important in many fields such as photodynamic therapy, sensor, storage, electronic devices, molecular recognition and catalysis (Li et al., 2004; Martelli et al., 2009; Melissa et al., 2001; Milanesio et al., 2002). Porphyrias are a group of rare diseases characterized by excessive production and excretion of porphyrins caused by enzyme deficiencies in the heme biosynthetic pathway (McCarroll, 1995; Wang et al., 2008). Consequently, the study of porphyrin compounds has been paid longstanding attention. However, determination of porphyrins in biological materials has long been bedeviled. Traditional methods used for the detection of porphyrin included spectrophotometry (Kufner et al., 2005), fluorometric method (Huie and Williams, 1989), high performance liquid chromatography (HPLC) (Bozek et al., 2005; Macours and Cotton, 2006), mass spectrometry (MS) (Luo et al., 1997), gas chromatography–mass spectrometry (GC–MS) (Ausió et al., 2000; Bu et al., 2003), capillary electrophoresis–fluorescence (CE–FL) (Wu et al., 1994). Due to the drawbacks of these techniques such as strenuosity, costliness, discontinuousness, complicated apparatus and usually requirement

* Corresponding author. Tel.: +86 931 7971276; fax: +86 931 7971323.
E-mail address: luxq@nwnu.edu.cn (X. Lu).

0956-5663/$ – see front matter © 2011 Elsevier B.V. All rights reserved.
doi:10.1016/j.bios.2011.06.043

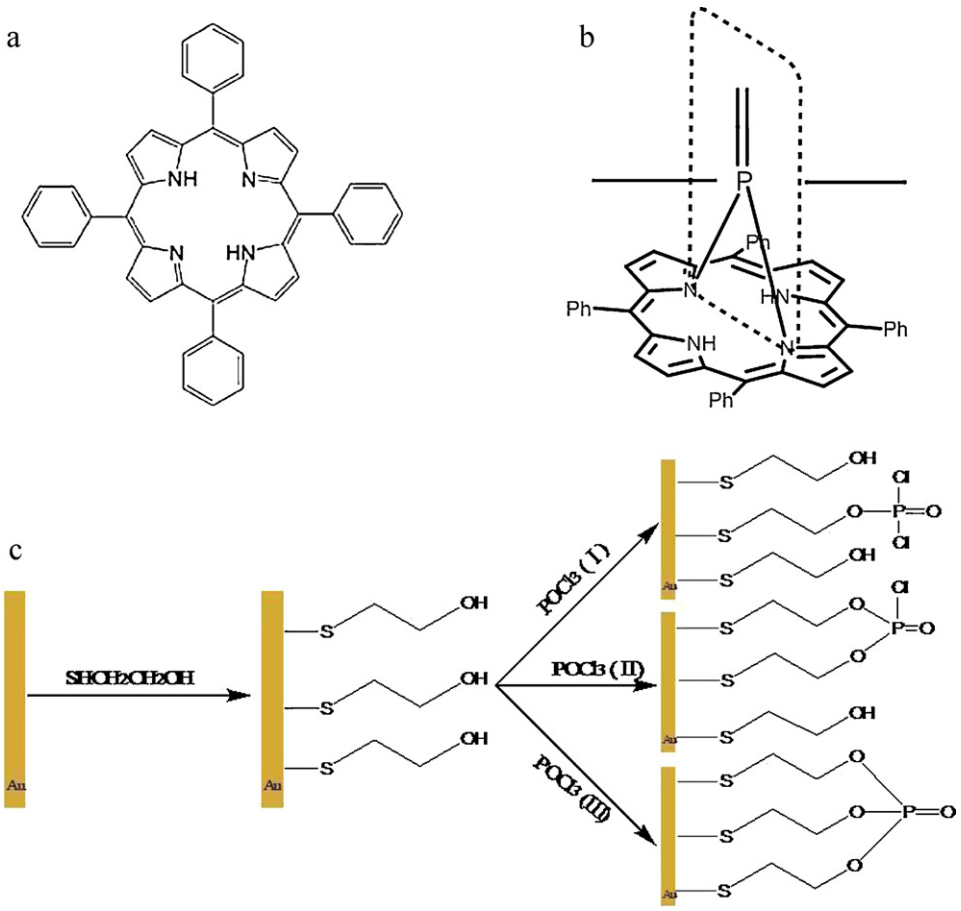

Scheme 1. (a) Structures of Tetraphenylporphyrin (TPP) molecular. (b) Reaction steps in the preparation of the phosphatized gold sheet (or electrode), for colorimetric and electrochemical detection of porphyrin. (c) P(V)–porphyrin complex.

of radio-labeled substrates, it is an open question about how to develop sensitive, simple, and economical methods for porphyrin detection.

In this work, a highly sensitively bifunctional sensor, a visual colorimetry biosensor as well as an electrochemistry sensor, aiming to determine the porphyrin applying phosphate-based self-assembled monolayer, was developed. The designed sensor was used to detect porphyrin with those two methods, which demonstrates some advantages: (i) it has fast response and high sensitiveness that the dramatic color changes from burgundy to dark green of porphyrin solution could be observed within 3 s. (ii) It is a stable fabric that can be used to detect porphyrin even after being stored for weeks in dichloromethane solution or air at 4 °C. (iii) This sensor with simple instrumentation is easy to miniaturizate and owns potential commercial application. In our research, detailed mechanism of sensing porphyrin applying phosphate-based self-assembled monolayer was proposed. Here, tetraphenylporphyrin (TPP) was selected in the research, and the designed sensor was successfully used for determination of pheophytin obtained from fresh spinach leaves.

2. Experimental

2.1. Reagents and materials

The tetraphenylporphyrin (TPP) (Scheme 1(a)) was synthesized and purified according to the method of previous literature (Lindsey et al., 1994; Zuo et al., 2006). Chlorophylls (Chls) from fresh spinach leaves was isolated and purified as previously described (Quach et al., 2004) and stored in the dark at 253 K.

Pheophytin was synthesized by adding acid to chlorophylls solution (Pennington et al., 1964). They were dissolved in dichloromethane. 2-Mercaptoethanol (2-ME) (Tianjin, China) and $POCl_3$ (Jiangsu, China) used without further treatment. Triethylamine (TEA) and Tetrahydrofuran (THF) were dried according to reported procedures (Becker et al., 2009). The reagents were of analytical grade and used as received. All solutions were prepared with doubly distilled water.

2.2. Apparatus

UV–vis absorption spectra were taken by absorption mode with a UV-1102 UV–vis spectrophotometer (Shanghai, China). The spectra were recorded in the 250–750 nm region. Electrochemical characterizations were performed by cyclic voltammetry (CV) and electrochemical impedance spectroscopy (EIS) (VMP2 Multi-potentiostat, Princeton Applied Research, USA) using a conventional three-electrode cell. Gold electrode (CHI101, Ø2 mm) was used as a working electrode, a platinum wire and an Ag/AgCl (KCl saturated) electrodes were used as counter and reference electrodes, respectively. The faradaic impedance spectra were recorded upon the application of the bias potentials in the frequency range from 10 kHz to 100 mHz, using an ac voltage of 0.005 V amplitude. The data obtained were analyzed using the fitting program in ZSimpWin software. All the measurements were carried out at ambient temperature (22 ± 2 °C).

2.3. Substrate and SAMs preparation

The gold sheet (or electrode) was prepared and modified using the procedures previously reported (Becker et al., 2009; Wang et al., 2009), but we increased the amount of phosphorus oxychloride to obtain the $-CH_2-O-P{=}OCl_2$ and $(-CH_2-O-)_2P{=}OCl$ (Scheme 1(c)). Functionalized gold sheet (or electrode) with phosphate groups was rinsed in copious amounts of chloroform, anhydrous ethanol and deionized water, respectively.

3. Results and discussion

3.1. Principle of sensing porphyrin via phosphate-based self-assembled monolayer

Because porphyrin is capable of specifically combining with phosphorus, herein, we utilize phosphate-based SAM sense porphyrin with two detection means. Scheme 1(c) shows the reaction steps of preparation of the phosphatized modified gold sheet (or electrode), which is easily prepared by simple and rapid synthetic procedure.

The first step involves the formation of a SAM of 2-ME on gold, exposing the hydroxyl (–OH) group as the nucleophiles at the surface of the SAM and the second step comprises the modification of the SAM with $POCl_3$ to yield phosphate moieties (Bent et al., 1994; Schilling et al., 1993). The three chlorines of $Cl_3P{=}O$ which could be replaced by surface hydroxyls are responsible for three styles of $Cl_3P{=}O$ reacting with hydroxyl (Bertilsson and Liedberg, 1993). Thus, a question of prime interest is whether the $Cl_3P{=}O$ molecule reacts with one surface hydroxyl to form $-CH_2-O-P{=}OCl_2$ species or to forms bridges like $(-CH_2-O-)_2P{=}OCl$ or $(-CH_2-O-)_3P{=}O$ between neighboring hydroxyl terminals. The likelihood of bridging is dependent on the distance between OH groups on the surface and the amount of phosphorus oxychloride. It is of interest to note that, when the phosphatized modified gold sheet (or electrode) immerses into dichloromethane solution containing TPP, a solution color change of burgundy to dark green can be observed in few minutes. In order to demonstrate that this phenomenon is not a protonation of TPP, triphenyl phosphate and triethyl phosphate were chosen and added to dichloromethane solution containing 1.0×10^{-4} M TPP, respectively. The former could react with TPP and solution color changed to dark green was observed, but the latter could not. We deduce that phosphonates could coordinate with TPP only if the axial ligands on phosphorus were readily removed, while triethyl phosphate could not react with TPP because of the ethyl hard to be removed. Thus, it implied that when all the three chlorines of $Cl_3P{=}O$ molecule were replaced by surface hydroxyls no reaction occurred with TPP solution. In addition, terephthaloyl chloride, methyl chloride and thionyl chloride were added to dichloromethane solution containing 1.0×10^{-4} M TPP, respectively, all of them could react with TPP solution. Based on above results, we conclude that only the first two reactions of functionalized gold sheet (or electrode) with phosphonates in Scheme 1(c) are attributed to the recognition of TPP and formed 1:1 cationic sitting-atop (SAT) complex P(V)–TPP (Scheme 1(b)) (Boeckl et al., 2000; Dehghani and Shaterian, 2008, 2009a,b; Inada et al., 2000). Here, we use a large excess of phosphorus oxychloride to reduce the formation of side product phosphoric acid anhydride (Spori et al., 2007).

3.2. Phosphate-based self-assembled monolayer characterization

The stepwise assembly of the layered functionalized electrode was traced by EIS. The electrochemical responses in each step were investigated to confirm the layer-by-layer assembly process.

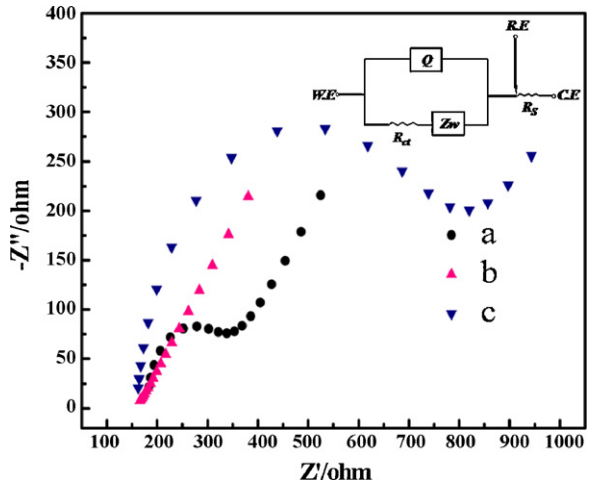

Fig. 1. (a) Cyclic voltammograms of bare Au electrode (curve 1), 2-ME–SAM electrode (curve 2) and phosphatized modified electrode (curve 3) in 5.0 mM $Fe(CN)_6^{3-/4-}$ with 0.1 M KCl as supporting electrolyte, with a scan rate of 50 mV/s. (b) Impedance measurements in the presence of 5.0 mM $Fe(CN)_6^{3-/4-}$ on (1) bare Au electrode, (2) 2-ME–SAM electrode and (3) phosphatized modified electrode. Inset: the equivalent circuit model used to obtain equations for Zre and Zim. R_s, R_{ct}, C_{dl} and Z_w represent the resistance of electrolyte, the charge transfer resistance, double-layer capacitance and the Warburg impedance, respectively.

Fig. 1 shows the faradaic impedance spectra presented as Nyquist plots upon the assembly of the two layers on the electrode. The bare Au electrode exhibits an almost straight line (curve 1) that is characteristic of a mass diffusional limiting electron-transfer process. Compared with the response on a bare gold electrode, $Fe(CN)_6^{3-/4-}$ exhibits better electron-transfer rate on a 2-ME modified gold electrode due to the attractive electrostatic forces between the protonated hydroxyl groups of 2-ME and $Fe(CN)_6^{3-/4-}$ (Hu et al., 1999). As the further reacting with $Cl_3P{=}O$, electron transfer was blocked, which is reflected by the appearance of the semicircle part on the spectrum. The surface coverage of saturated phosphate-based SAM was also estimated using a method reported by Weisshaar et al. (Weisshaar et al., 1993) The charge under a desorption wave was used to provide a measure of the surface coverage of SAMs. And the surface coverage Γ (mol/cm^2) was calculated, on the basis of the relationship $\Gamma = Q/nFA$ (where Q is the total charge (C), A is the electrode surface area (cm^2), and n and F have their usual electrochemical meanings). By integrating the charges (Q) passing on the cathodic wave, the estimated surface coverage for the phosphate-based SAM was 2.43×10^{-11} mol/cm^2.

3.3. Visual colorimetric detection of pophyrin

Visual colorimetry is a widely used way in biochemistry to determine the concentration of colored compounds and to evaluate the intensity of the color in solution (Brotto et al., 2010; Feng et al., 2010; Li et al., 2010). Here, employing visual colorimetry to detect porphyrin has advantages of rapidity, simpleness, inexpensiveness and high sensitiveness. Different concentrations of TPP were analyzed via monitoring visible color change of the colored product P(V)–TPP complex (Fig. 2(a)).

When phosphatized modified gold sheet (or electrode) immerses into 0.5 mL dichloromethane solution containing 1.0×10^{-4} M TPP, a solution color change from burgundy to dark green could be observed within 3 s. With the increasing concentrations and volume of TPP solution, the more time will be needed in the coordination between TPP and phosphate on gold sheet (or electrode) which leads to lower change of TPP solution color. These results show that when phosphate binding sites become saturated no color change of TPP solution occurs. The mod-

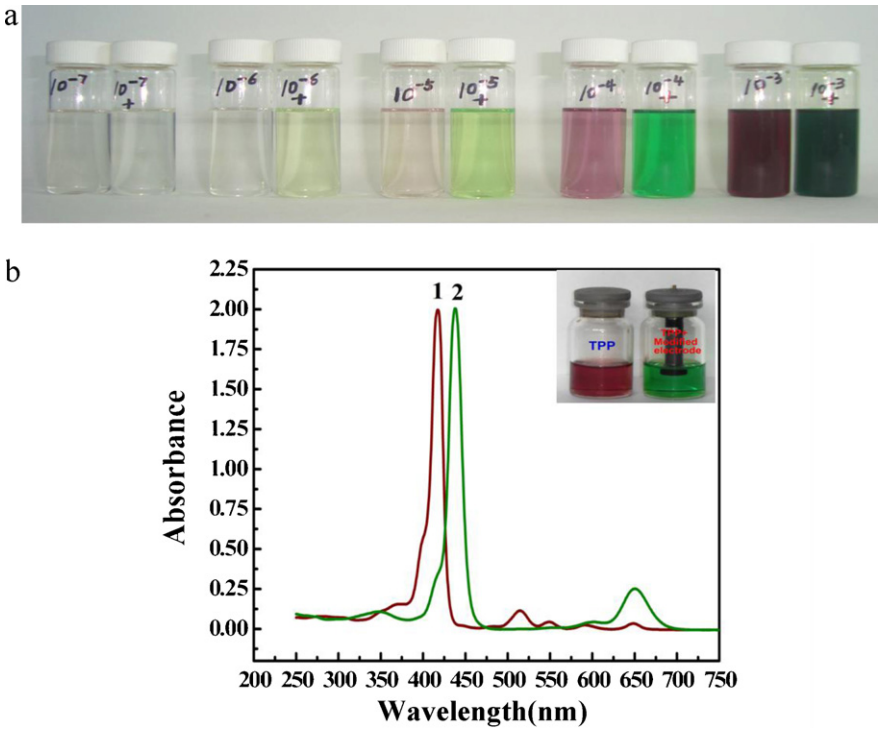

Fig. 2. (a) Different concentrations of TPP before and after reacting with functionalized gold sheet: 1.0×10^{-7} M, 1.0×10^{-6} M, 1.0×10^{-5} M, 1.0×10^{-4} M and 1.0×10^{-3} M from left to right. (b) Absorption spectra of TPP before (1) and after (2) reacting with functionalized gold sheet (or electrode) in dichloromethane solution.

ified gold sheet (or electrode) was washed carefully after each incubation step. The detection limit for TPP analysis with visual colorimetry is 1.0×10^{-6} M. The above observations demonstrate the phosphate-based self-assembled monolayer can serve as a novel visual colorimetric sensor for sensitive porphyrin detection.

Fig. 2(b) shows a UV–vis spectrum of TPP and corresponding SAT P(V)–TPP complex which indicates complexation between TPP and phosphate on electrode. The TPP solution shows a strong Soret band at 419 nm and four weaker Q bands in the region between 500 and 700 nm, which are typical bands of a free base porphyrin (Meot-Ner and Adler, 1975; Stone and Fleischer, 1968). These bands arise from the π–π^* transition of the macrocycle (Zhang et al., 1997). In the case of the corresponding SAT P(V)–TPP complex, the Soret band at the 419 nm peak drastically decreased and appeared at 441 nm, and the Q band at the 650 nm increased. The red shift by 22 nm of the Soret band indicates that the interaction of phosphatized modified electrode with TPP causes distortion of the TPP plane and leads to the resonance between aryl groups and TPP core increase, to form the 1:1 cationic SAT complex (Dehghani and Shaterian, 2009b).

3.4. EIS detection of porphyrin

The EIS is a powerful technique for studying electric and dielectric behavior of electrode materials and is superior to other electrochemical techniques (Boubour and Lennox, 2000; Love et al., 2005; Peng et al., 2006). It has been employed in many biosensing (Eugenii and Itamar, 2003; Gao et al., 2011) and immunosensing (Bourigua et al., 2010; Mantzila et al., 2008) systems as a transduction technique. Likewise, quantitative TPP analysis utilizing phosphate-based self-assembled monolayer is also performed by the EIS method. Fig. 3(a) shows the faradaic impedance spectra were obtained on phosphate functionalized electrode in the different concentrations of TPP solution for fixed incubation time,

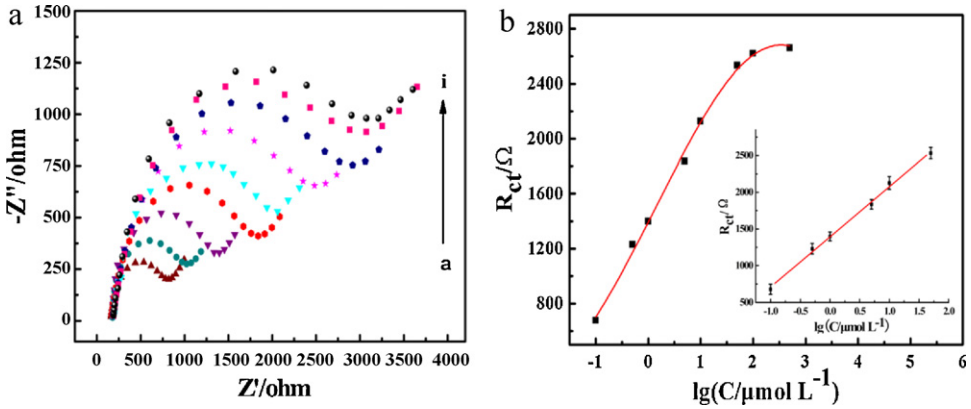

Fig. 3. (a) Impedance response in the presence of 5.0 mM $Fe(CN)_6^{3-/4-}$ on functionalized Au electrode before and after incubation of the electrode for 3 min in various concentrations of TPP: 1.0×10^{-7} M, 5.0×10^{-7} M, 1.0×10^{-6} M, 5.0×10^{-6} M, 1.0×10^{-5} M, 5.0×10^{-5} M, 1.0×10^{-4} M, and 5.0×10^{-4} M from bottom to top. (b) Plot for TPP concentration versus resistance value (R_{ct}). Inset: the linear relation between TPP concentrations and the resistance value (R_{ct}).

Table 1
Results of porphyrin in pheophytin sample.

Sample	Results by proposed method Results by UV					
	Found (μmol L^{-1})	Added (μmol L^{-1})	Total (μmol L^{-1})	Recovery (%)	RSD (%) (n = 4)	Found (μmol L^{-1})
Pheophytin	0.24	0.12	0.35	91.7	2.07	0.22
	0.23	0.24	0.46	95.8	2.56	0.20
	0.22	0.36	0.60	105.6	1.98	0.23
	0.23	0.48	0.68	93.8	2.25	0.22

3 min. The resistance value (R_{ct}) gradually increased along with the increase of TPP concentration in certain range (Fig. 3(b)).

The R_{ct} is linearly dependent on the logarithm of TPP concentration in the range from 1.0×10^{-7} M to 5.0×10^{-5} M (R = 0.9984). That R_{ct} reaches a saturation value at high TPP concentration indicates that the binding sites become saturated, and there is no more phosphate site for further TPP. This result is consistent with the colorimetry described above.

4. Application

To demonstrate the application potential of our bifunctional sensor probe in practical analysis, we applied phosphate-based self-assembled monolayer to detect pheophytin obtained from spinach leaves. The measured pheophytin contents are listed in Table 1. The results obtained by using the proposed method were in good agreement with results obtained by using the method of spectrophotometry, and the recovery was from 91.7 to 105.6%. The developed sensor was free of interferences of carotenol, carotene, chlorophyll and vitamins.

5. Conclusions

In summary, the ability of phosphate groups to form strong bonds with porphyrin has provided a strategy to detect porphyrin utilizing SAMs. Herein, a feasible method of fabricating porphyrin sensor was developed by 2-mercaptoethanol (2-ME) SAM modified gold sheet (or electrode) then functionalized with phosphate groups, and porphyrin combining with phosphorus formed 1:1 cationic SAT type of P(V)–porphyrin complex. Excellent detectability and selectivity achieved in our experiment demonstrated the possibility of using phosphate-based self-assembled monolayer for detection of porphyrin by visual colorimetry and electrochemical methods. The modified gold sheet (or electrode) retained stable for analysis of porphyrin after being stored for weeks in dichloromethane solution or air at 4 °C. The practical application by using the designed sensor to determine pheophytin obtained from fresh spinach leaves received satisfactory results. Compared with the traditional method to detect porphyrin, the proposed method can be very easily operated and less costly. Such an efficient bifunctional biosensor offers great potential in quantitative of porphyrin levels in biological and medical systems, and development of an allochroic product, likewise pH test paper is promising.

Acknowledgements

This work was supported by the Natural Science Foundation of China (no. 20775060, 20875077 and 20927004), the Natural Science Foundation of Gansu (nos. 0701RJZA109, 0803RJZA105), Key Progress of the Education Committee (08zx-07) of Gansu and the Key Laboratory of Polymer Materials of Gansu Province, China.

Appendix A. Supplementary data

Supplementary data associated with this article can be found, in the online version, at doi:10.1016/j.bios.2011.06.043.

References

Ausió, X., Grimalt, J.O., Ozalla, D., Herrero, C., 2000. Anal. Chem. 72, 4874–4877.
Becker, A., Tobias, H., Mandler, D., 2009. Anal. Chem. 81, 8627–8631.
Bent, S.F., Schilling, M.L., Wilson, W.L., Katz, H.E., Harris, A.L., 1994. Chem. Mater. 6, 122–126.
Bertilsson, L., Liedberg, B., 1993. Langmuir 9, 141–149.
Boeckl, M.S., Bramblett, A.L., Hauch, K.D., Sasaki, T., Ratner, B.D., Rogers, J.W., 2000. Langmuir 16, 5644–5653.
Boubour, E., Lennox, R.B., 2000. Langmuir 16, 7464–7470.
Bourigua, S., Hnaien, M., Bessueille, F., Lagarde, F., Dzyadevych, S., Maaref, A., Bausells, J., Errachid, A., Renault, N.J., 2010. Biosens. Bioelectron. 26, 1278–1282.
Bozek, P., Hutta, M., Hrivnáková, B., 2005. J. Chromatogr. A 1084, 24–32.
Brotto, L., Battistutta, F., Tat, L., Comuzzo, P., Zironi, R., 2010. J. Agric. Food Chem. 58, 3567–3572.
Bu, W., Myers, N., McCarty, J.D., O'Neill, T., Hollar, S., Stetson, P.L., Sved, D.W., 2003. J. Chromatogr. B 783, 411–423.
Carroll, R.L., Christopher, B.G., 2002. Angew. Chem. Int. Ed. 41, 4378–4400.
Chiu, C.-S., Lee, H.-M., Gwo, S., 2009. Langmuir 26, 2969–2974.
Dehghani, H., Shaterian, M., 2008. Polyhedron 27, 3263–3266.
Dehghani, H., Shaterian, M., 2009a. Inorg. Chim. Acta 362, 2868–2871.
Dehghani, H., Shaterian, M., 2009b. Inorg. Chim. Acta 362, 5151–5154.
Eugenii, K., Itamar, W., 2003. Electroanalysis 15, 913–947.
Feng, L., Musto, C.J., Suslick, K.S., 2010. J. Am. Chem. Soc. 132, 4046–4047.
Fragoso, A., Laboria, N., Latta, D., O'Sullivan, C.K., 2008. Anal. Chem. 80, 2556–2563.
Gao, Q., Zhang, W., Guo, Y., Qi, H., Zhang, C., 2011. Electrochem. Commun. 13, 335–337.
Hu, X.-Y., Xiao, Y., Chen, H.-Y., 1999. J. Electroanal. Chem. 466, 26–30.
Huie, C.W., Williams, W.R., 1989. Anal. Chem. 61, 2288–2292.
Inada, Y., Nakano, Y., Inamo, M., Nomura, M., Funahashi, S., 2000. Inorg. Chem. 39, 4793–4801.
Kufner, G., Schlegel, H., Jäger, R., 2005. Clin. Chem. Lab. Med. 43, 183–191.
Li, Q., Mathur, G., Gowda, S., Surthi, S., Zhao, Q., Yu, L., Lindsey, J.S., Bocian, D.F., Misra, V., 2004. Adv. Mater. 16, 133–137.
Li, T., Wang, E., Dong, S., 2010. Anal. Chem. 82, 1515–1520.
Lindsey, J.S., MacCrum, K.A., Tyhonas, J.S., Chuang, Y.Y., 1994. J. Org. Chem. 59, 579–587.
Love, J.C., Estroff, L.A., Kriebel, J.K., Nuzzo, R.G., Whitesides, G.M., 2005. Chem. Rev. 105, 1103–1170.
Luo, J., Lamb, J.H., Lim, C.K., 1997. J. Pharm. Biomed. Anal. 15, 1289–1294.
Macours, P., Cotton, F., 2006. Clin. Chem. Lab. Med. 44, 1433–1440.
Mantzila, A.G., Maipa, V., Prodromidis, M.I., 2008. Anal. Chem. 80, 1169–1175.
Martelli, C., Canning, J., Reimers, J.R., Sintic, M., Stocks, D., Khoury, T., Crossley, M.J., 2009. J. Am. Chem. Soc. 131, 2925–2933.
McCarroll, N.A., 1995. Anal. Chem. 67, 425–428.
Melissa, L.M., Maria del Pilar, M., SonBinh, T.N., Joseph, T.H., 2001. Angew. Chem. Int. Ed. 40, 4239–4242.
Meot-Ner, M., Adler, A.D., 1975. J. Am. Chem. Soc. 97, 5107–5111.
Milanesio, M.E., Miguel, G., Luis, A.O., Leonides, S., Juana, J.S., Edgardo, N.D., 2002. J. Phys. Org. Chem. 15, 844–851.
Panagopoulou, M.A., Stergiou, D.V., Roussis, I.G., Prodromidis, M.I., 2010. Anal. Chem. 82, 8629–8636.
Peng, D.K., Yu, S.T., Alberts, D.J., Lahann, J., 2006. Langmuir 23, 297–304.
Pennington, F.C., Strain, H.H., Svec, W.A., Katz, J.J., 1964. J. Am. Chem. Soc. 86, 1418–1426.
Quach, H.T., Steeper, R.L., Griffin, G.W., 2004. J. Chem. Educ. 81, 385.
Rezaei, B., Majidi, N., Rahmani, H., Khayamian, T., 2011. Biosens. Bioelectron. 26, 2130–2134.
Schönherr, H., Vancso, G.J., Huisman, B.-H., van Veggel, F.C.J.M., Reinhoudt, D.N., 1997. Langmuir 13, 1567–1570.
Schilling, M.L., Katz, H.E., Stein, S.M., Shane, S.F., Wilson, W.L., Ungashe, S.B., Taylor, G.N., Putvinski, T.M., Chidsey, C.E.D., Buratto, S., 1993. Langmuir 9, 2156–2160.
Seitz, O., Dai, M., Aguirre-Tostado, F.S., Wallace, R.M., Chabal, Y.J., 2009. J. Am. Chem. Soc. 131, 18159–18167.
Spori, D.M., Venkataraman, N.V., Tosatti, S.G.P., Durmaz, F., Spencer, N.D., Zürcher, S., 2007. Langmuir 23, 8053–8060.

Stettner, J., Winkler, A., 2010. Langmuir 26, 9659–9665.
Stone, A., Fleischer, E.B., 1968. J. Am. Chem. Soc. 90, 2735–2748.
Sun, H., Bu, W., Li, Y., Li, H., Wu, L., Sun, C., Dong, B., Dou, R., Chi, L., Schaefer, A., 2008. Langmuir 24, 4693–4699.
Wang, Q., Zhi, F., Wang, W., Xia, X., Liu, X., Meng, F., Song, Y., Yang, C., Lu, X., 2009. J. Phys. Chem. C 113, 9359–9367.
Wang, Y., Gatti, P., Sadilek, M., Scott, C.R., Turecěk, F., Gelb, M.H., 2008. Anal. Chem. 80, 2599–2605.
Weisshaar, D.E., Walczak, M.M., Porter, M.D., 1993. Langmuir 9, 323–329.
Wu, N., Li, B., Sweedler, J.V., 1994. J. Liq. Chromatogr. 17, 1917–1927.
Zhang, Z., Verma, A.L., Yoneyama, M., Nakashima, K., Iriyama, K., Ozaki, Y., 1997. Langmuir 13, 4422–4427.
Zhi, F., Lu, X., Yang, J., Wang, X., Shang, H., Zhang, S., Xue, Z., 2009. J. Phys. Chem. C 113, 13166–13172.
Zuo, G., Lu, X., Xue, Z., Lv, B., Wang, Y., Kang, J., 2006. Synth. React. Inorg. M. 36, 589–594.